FACE-UP CHEMICAL MECHANICAL POLISHING: KINEMATICS AND MATERIAL REMOVAL RATE

by

Marvin Bryan Shieh

Submitted to the Department of Mechanical Engineering
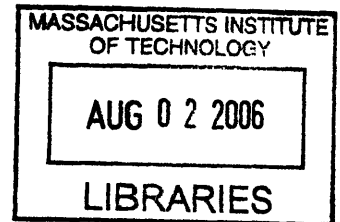in Partial Fulfillment of the Requirements for the Degree of

Bachelor of Science

at the

Massachusetts Institute of Technology

June 2006

© 2006 Marvin Bryan Shieh
All Rights Reserved

Signature of Author: _____
Marvin Bryan Shieh
Department of Mechanical Engineering
May 12, 2006

Certified by: _____
Jung-Hoon Chun
Professor of Mechanical Engineering
Thesis Supervisor

Certified by: _____
Nannaji Saka
Research Affiliate, Department of Mechanical Engineering
Thesis Supervisor

Accepted by: _____
John H. Lienhard V
Professor of Mechanical Engineering
Chairman, Undergraduate Thesis Committee

FACE-UP CHEMICAL MECHANICAL POLISHING: KINEMATICS AND MATERIAL REMOVAL RATE

by

Marvin Bryan Shieh

Submitted to the Department of Mechanical Engineering
on May 12, 2006 in Partial Fulfillment of the Requirement for the Degree of
Bachelor of Science in Mechanical Engineering

ABSTRACT

A working prototype *face-up* CMP tool has successfully been completed. Experiments conducted on the *face-up* CMP machine qualitatively correspond with the theoretical polishing model. Discrepancies in data from the theoretical model could potentially be caused by non-uniform loading of the polishing pad and uneven distribution of slurry over the pad due to the edge effects on fluid flow. Despite the discrepancies, experimental data suggest that the theoretical model used to describe blanket wafer polishing by the *face-up* CMP tool is at least partially valid.

Thesis Supervisor: Dr. Jung-Hoon Chun
Title: Professor of Mechanical Engineering

Thesis Supervisor: Dr. Nannaji Saka
Title: Research Affiliate, Department of Mechanical Engineering

2

Acknowledgments

I would like to thank my advisors, Prof.. Jung-Hoon Chun and Dr. Nannaji Saka, for their guidance and assistance toward the completion of this thesis. With their help, I have learned a great many things about persistence, creativity, drive to succeed, and even humility. .

Without the patience and understanding of my advisors, I would not have begun to understand how to advise myself.

I also want to thank my family for being the ever-solid foundation from which I continue to find inspiration and strength. Without my family, none of this could have happened.

Table of Contents

List of Figures

5

List of Tables

1. Introduction

Chemical-mechanical planarization or polishing (CMP) is a process used in semiconductor fabrication for planarizing the surface of an in-process semiconductor wafer. The surface of the silicon dioxide coating on silicon wafer is chemically etched and an electrically conducting coating, in the present case copper, is applied over the wafer by vapor deposition or electroplating. The resulting surface is then polished, leaving copper filled trenches, as shown in Figure 1[1].
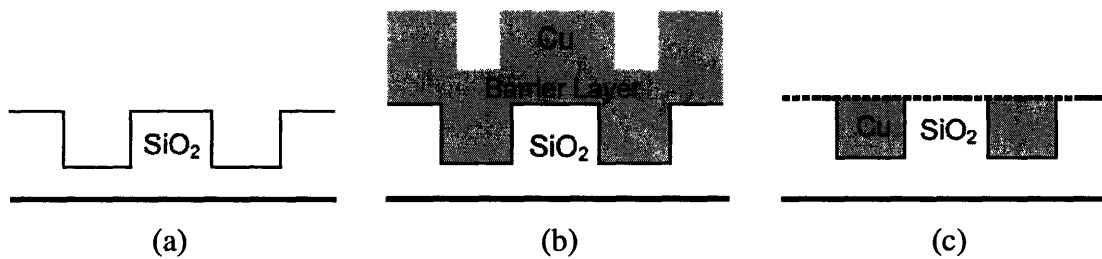
Figure 1: (a) Patterned silicon dioxide surface, (b) vapor deposited or electroplated Cu layer, and (c) ideal planarized surface by Cu CMP.

Traditionally, the wafer is held with its patterns *face-down* in a rotating wafer carrier and pressed against a much larger polishing pad, as show in Figure 2(a)[1]. Slurry is then fed onto the pad outside the wafer and is drawn into the wafer/pad interface as the wafer and pad are rotated relative to each other. Ideally, the end result should be planarized wafer topography. This however is often not the case, for it is virtually impossible to achieve a high degree of wafer-scale polishing uniformity using current conventional CMP tools. Conditions such as pressure, relative velocity, and slurry distribution all have an effect on the material removal rate of the substrate being polished off the wafer. In conventional *face-down* CMP the wafer is in contact with the pad at all times; so any non-uniformity of these variables could cause the wafer to be unevenly polished.

The *face-up* scheme flips the wafer downside up and uses a smaller pad. The pad is perforated and slurry is fed into a retaining vessel to allow a constant slurry flow rate across the pad, as shown in Figure 2(b).

7
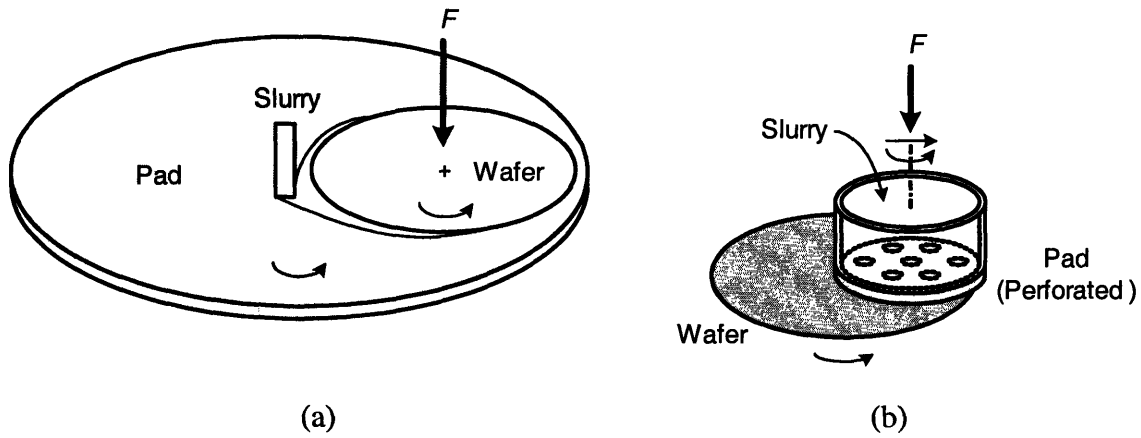
Figure 2: Schematics of (a) traditional *face-down*, and (b) novel *face-up* CMP tools.

Primary advantages of the *face-up* over *face-down* CMP include the following: First, polishing a wafer uniformly is now more controllable for the pad does not cover the entire wafer. As the polished region grows from the center outward, the polishing cup is moved in response to the polished region to prevent overpolishing. Second, the pressure applied by the pad is much easier to control as the polishing pad is smaller than the wafer. Third, the material removal rate of the wafer substrate can be more easily controlled because the slurry is evenly distributed over the pad through the perforations, as opposed to the conventional method of feeding the slurry from outside the wafer. With a more uniform slurry distribution over the polishing pad now, the kinematics of the system will have a greater effect on the rate of polishing.

2. Theory of Face-Up Polishing

2.1 Pad/Wafer Contact Geometry

Because the entire wafer is not always in contact with the polishing pad in the *face-up* setup, the "contact angle", θ_c, shown in Figure 3, directly affects the material removal rate at a given radius of the wafer. An expression containing the contact angle can be defined with the distance between the centers of the wafer and pad, r_{cc}, the radius of the wafer, r_w, the pad radius, r_p, and the angle of contact, θ_c

$$r_p^2 = r^2 + r_{cc}^2 - 2r_{cc}\cos\theta_c.$$ (1)
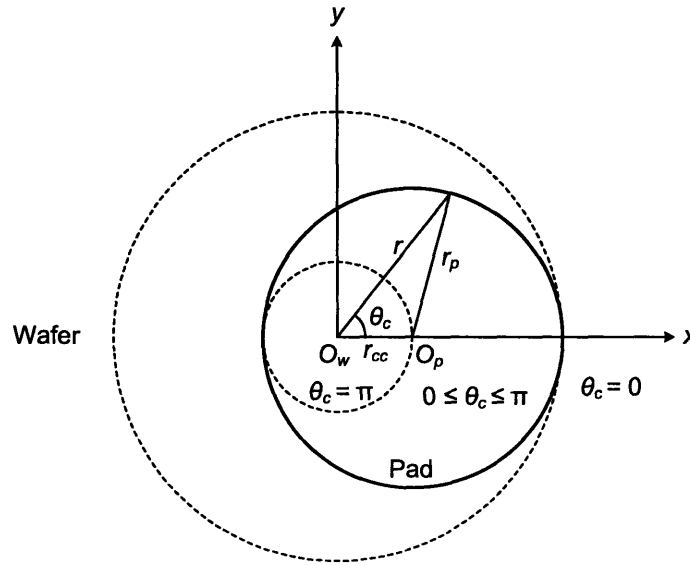
Figure 3: Definition of pad "contact angle", θ_c, in the *face-up* CMP scheme.

2.2 Kinematics

Figure 4 shows the coordinate system for the proposed *face-up* kinematics. The velocity of the wafer relative to the pad, v_R, at point $P(r, \theta)$ is calculated in the wafer coordinate system as [2]:

$$v_R(r,\theta) = -[(\omega_w - \omega_p)r\sin\theta + v_{cc}]e_x + [(\omega_w - \omega_p)r\cos\theta + \omega_p r_{cc}]e_y.$$ (2)

9

where ω_w and ω_p are the angular velocities of the wafer and the pad, respectively. The magnitude of the relative velocity, $v_R(r, \theta)$, yields the expression:

$$v_R(r,\theta) = \sqrt{[(\omega_w - \omega_p)r\sin\theta + v_{cc}]^2 + [(\omega_w - \omega_p)r\cos\theta + \omega_p r_{cc}]^2} \ . \tag{3}$$
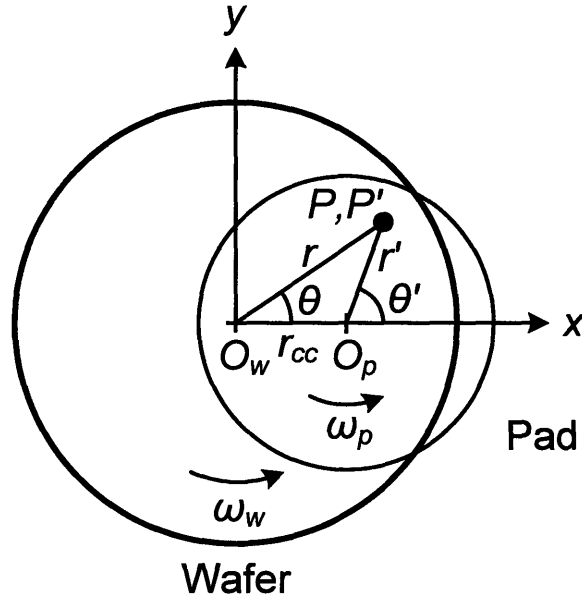
Figure 4: Cartesian and polar coordinate systems for *face-up* CMP with origin at the center of the wafer.

When the translational velocity is zero, $v_{cc} = 0$, the relative velocity can then be expressed as:

$$v_R(r,\theta) = \sqrt{[(\omega_w - \omega_p)r]^2 + (\omega_p r_{cc})^2 + 2(\omega_w - \omega_p)\omega_p r_{cc} r\cos\theta} \ . \tag{4}$$

Additionally, if the wafer and the pad are rotated at the same velocity, $\omega_w = \omega_p = \omega$, and there is no horizontal translation of the polishing cup, $v_{cc} = 0$, Eq. 4 simplifies to

$$v_R = \omega\, r_{cc} \ . \tag{5}$$

2.3 Material Removal Rate

The material removal rate of copper on the surface of the wafer is governed by the duration of polishing t, applied pressure p, relative velocity v_R, and Preston constant k_p, and is expressed by the Preston equation [3]:

$$\left|\frac{dh}{dt}\right| = k_p \cdot p \cdot v_R .$$

(6)

The Preston equation pertains to local material removal rate. The material removed Δh at $P(r)$ for one wafer rotation can be expressed as follows (given $dt = d\theta / \omega_w$ and $\Delta t = 2\pi / \omega_w$)

$$\Delta h = \int_0^{\Delta t} \left|\frac{dh}{dt}\right| dt = \int_0^{2\pi} \frac{1}{\omega_w} \left|\frac{dh}{dt}\right| d\theta .$$

(7)

Unlike the traditional *face-down* CMP setups, a point on the wafer in the *face-up* CMP scheme is not always in contact with the polishing pad. When the point on the wafer is in contact with the polishing pad the material removal rate follows the Preston equation; otherwise the material removal rate is zero. The Preston constant as well as pressure may not actually be constant across the entire surface of the wafer. For simplicity, however, we assume in this analysis that they are both constant in the region being polished.

As seen in Fig. 3, the contact angle θ_c directly affects the material removal rate. Material removed, Δh, can be rewritten in terms of the contact angle and the Preston equation as:

$$\Delta h(r) = \int_{-\theta_{c1}}^{\theta_{c2}} \frac{1}{\omega_w} k_p p v_R \, d\theta .$$

(8)

Substituting v_R in Eq. 8 with Eq. 3 yields

$$\Delta h(r) = k_p p \int_{-\theta_{c1}}^{\theta_{c2}} \frac{1}{\omega_w} \sqrt{[(\omega_w - \omega_p)r\sin\theta + v_{cc}]^2 + [(\omega_w - \omega_p)r\cos\theta + \omega_p r_{cc}]^2} \, d\theta .$$

(9)

11

While the wafer and pad velocities, ω_w and ω_p, and center to center distances, r_{cc}, can change through the duration of polishing, further analysis will rely on these variables being time-independent, i.e.,

$$\omega_w(t) = \omega_w$$
$$\omega_p(t) = \omega_p \ .$$
$$r_{cc}(t) = r_{cc}$$

(10)

Translational velocity of the pad is also assumed to be zero, $v_{cc}(t) = 0$, representing a stationary pad. With these new parameters for a stationary pad, Eq. 9 becomes

$$\Delta h(r) = k_p p \int_0^{\theta_{c2}} \frac{2}{\omega_w} \sqrt{[(\omega_w - \omega_p)r\sin\theta]^2 + [(\omega_w - \omega_p)r\cos\theta + \omega_p r_{cc}]^2} \ d\theta .$$

(11)

The material removed can be defined in terms the of the radius of the wafer, r, and the number of wafer revolutions, n:

$$\Delta h = \Delta h(r,n)$$

(12)

Similarly, the material removed at the center of the wafer in one revolution can be expressed as

$$\Delta h(0,1) = k_p p \cdot \pi r_{cc}(0) \cdot \frac{\omega_p(0)}{\omega_w(0)}$$

(13)

Thus, for a stationary pad with time-independent rotational speeds, the material removed at any radius r can be expressed in dimensionless form as

$$\Delta h * (r,n) \equiv \frac{\Delta h(r,n)}{\Delta h(0,1)}$$

$$\Delta h * (r) = \frac{2}{\pi} \int_0^{\theta_{c2}} \frac{2}{\omega_w} \sqrt{\left[(\frac{\omega_w}{\omega_p} - 1)\frac{r}{r_{cc}}\sin\theta\right]^2 + \left[(\frac{\omega_w}{\omega_p} - 1)\frac{r}{r_{cc}}\cos\theta + 1\right]^2} \ d\theta$$

(14, 15)

Figure 5 shows $\Delta h*$ for various wafer and pad rotational speed ratios versus dimensionless radial position on the wafer. It may be noted that $\Delta h*$ is the normalized polishing rate, i.e., the material removal rate any dimensionless radius r/r_w divided by

12

material removal rate at the center of the wafer. If the pad is stationary and the angular velocities are constant, Δh^* is independent of time.
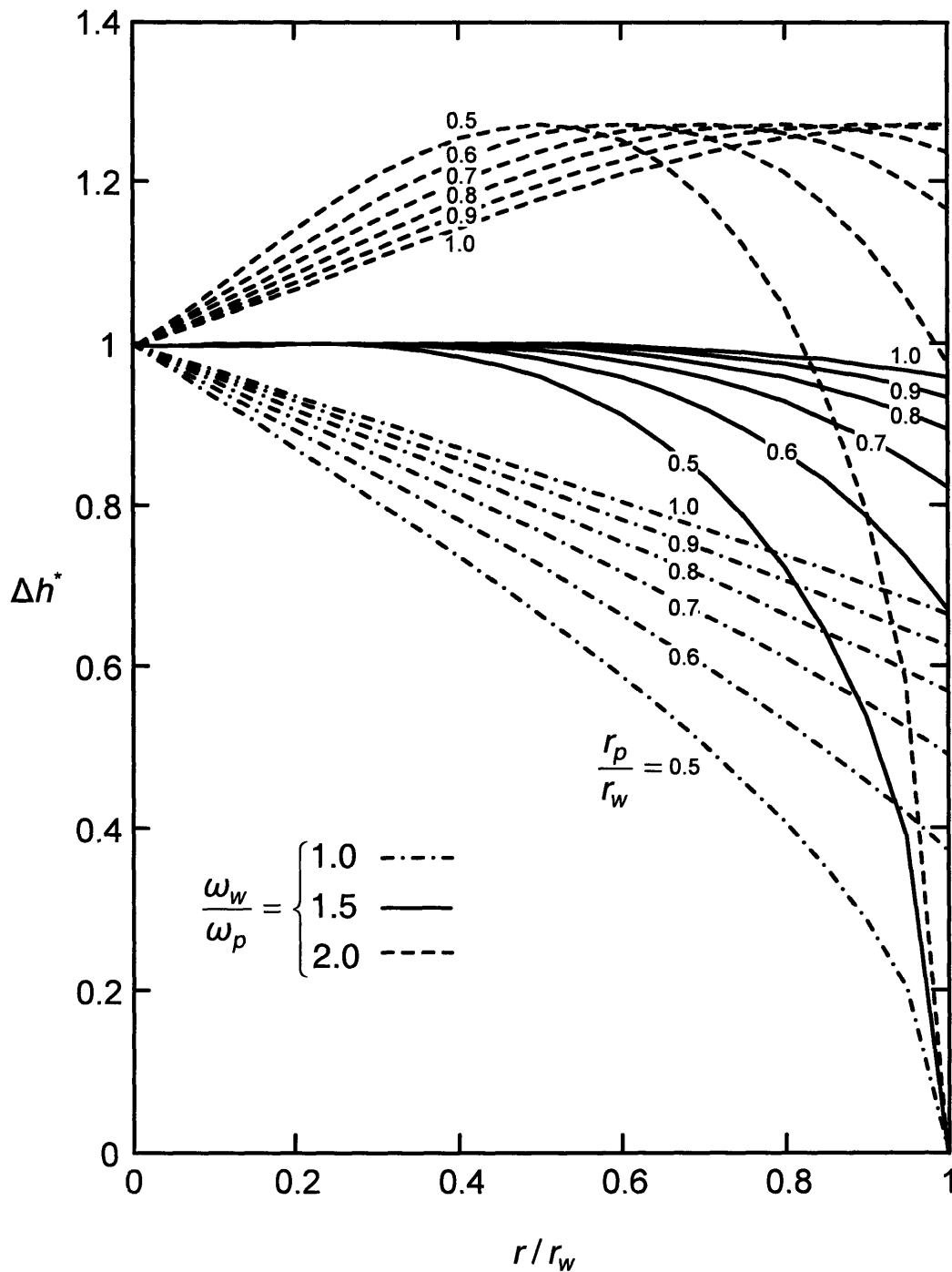

Figure 5: Δh^* versus r/r_w plots for various ω_w/ω_p and r_p/r_w values.

3. Apparatus

The experimental setup, a *face-up* prototype CMP tool, employed for polishing blanket wafers is shown in Figure 6. A brief description of the individual components follows.
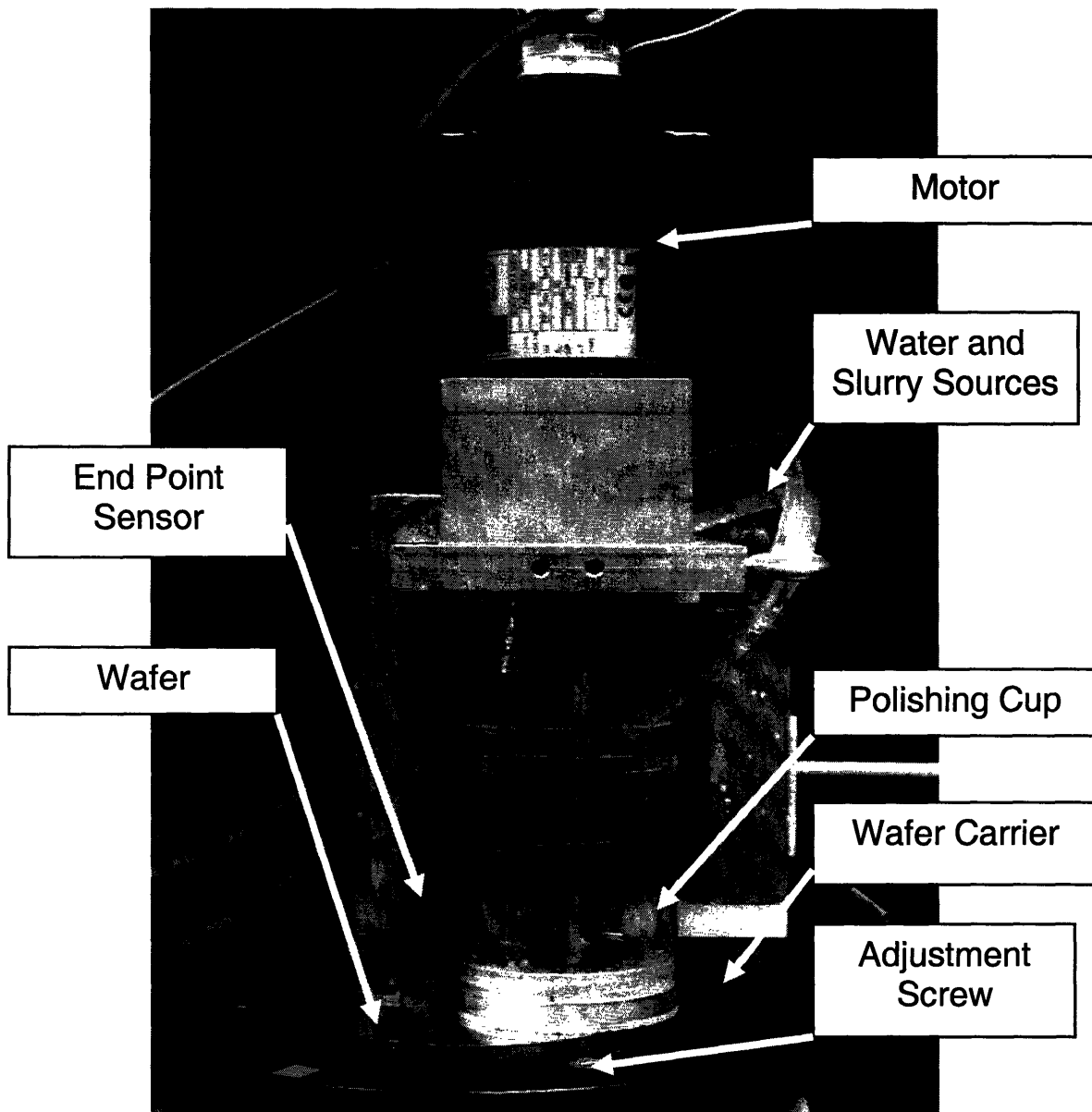

Figure 6: Prototype of *face-up* CMP machine.
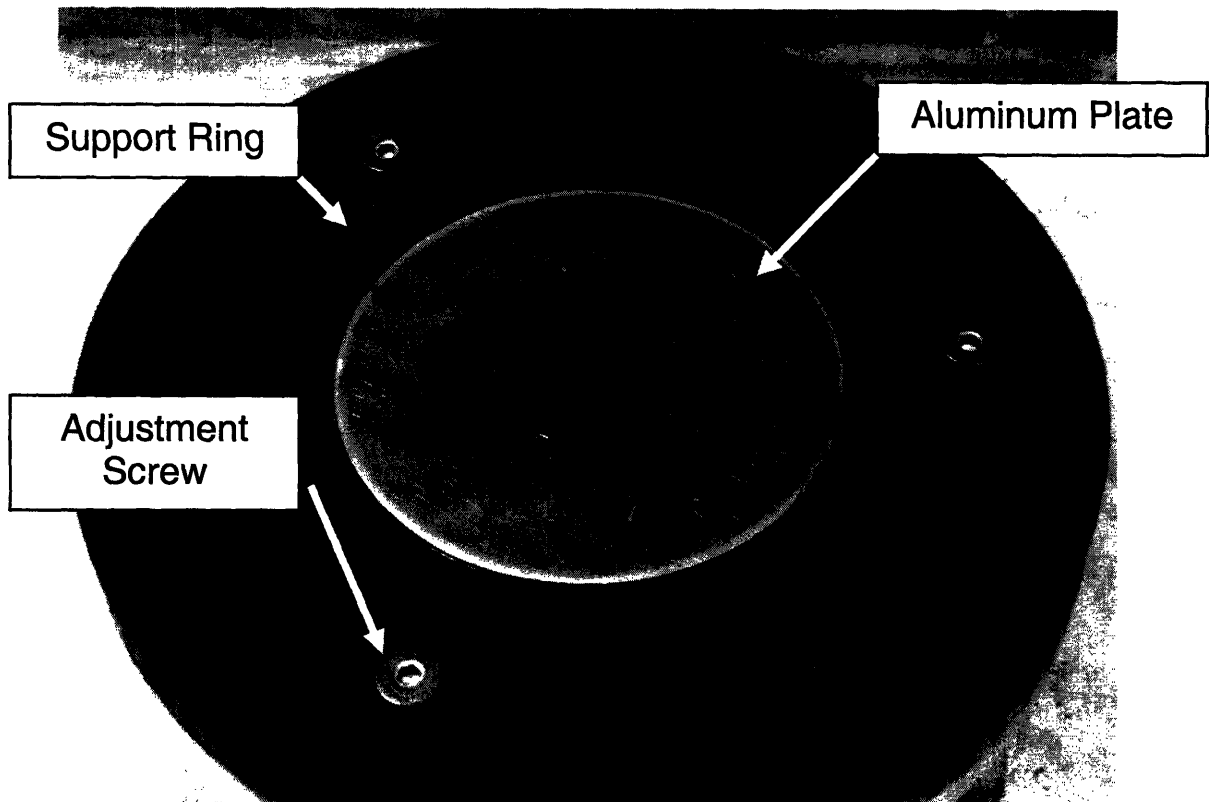
Figure 7: Wafer carrier without the wafer.

3.1 Wafer Carrier

The wafer is held in place face-up on the wafer carrier by means of a vacuum. A thin layer of oil is applied to the backside of the wafer and placed upon a perforated circular aluminum plate, shown in Figure 7. When the vacuum is drawn, the wafer tends to conform to the surface which it is on, assuming the stresses do not exceed the fracture stress of the silicon. Since the wafer only has at most a 1.5-μm thick layer of copper, the flatness of the aluminum plate is important so that the wafer is likewise very flat. The aluminum plate in this setup was machined and polished to have a surface variation of no more than 5 μm over the entire diameter of the plate.

Since the polishing pad, attached to the slurry cup, does not rest entirely on the wafer, a support ring (Fig. 7) is necessary to bear the rest of the load and to prevent excessive slurry leakage. Leveling of the support ring is done with three adjustment screws, shown in Figure 7, and verified using a dial indicator with a resolution of 5 ± 2.54 μm.

15

3.2 Polishing Cup and Pad

The polishing mechanics of the *face-up* CMP machine, as with any machinery, involves some level of misalignment and runout. In order to better accommodate for these irregularities in the polishing mechanics, the cup utilizes a gimbal so that the application of normal force and torque are intrinsically decoupled. The shaft provides the normal force while the pins orthogonal to the shaft provide the torque to rotate the cup and pad. By having the rounded end of the shaft interface with a cone, shown in Figure 8(a), the cup is able to account for small deflections due to runout.

(a)   (b)
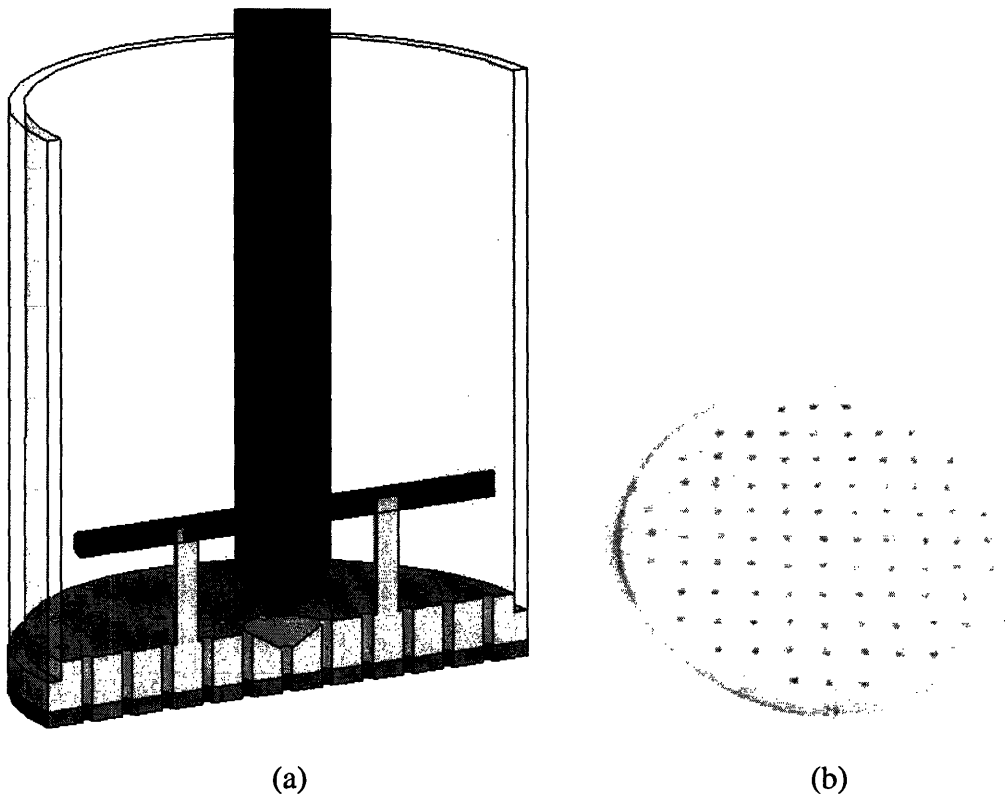
Figure 8: (a) 3D CAD of polishing cup with perforated bottom and (b) polishing pad.

The polishing pad, shown in Figure 8(b), consists of two layers. The top layer of the pad, the layer that contacts the wafer, is a hard and porous material relative to the softer lower layer. The purpose of the bottom layer is to account for small deflections during the polishing process.

16

3.3 End-Point Sensing

During the polishing process, it is useful to monitor the polished state of the wafer to prevent over-polishing. End-point sensing for conventional *face-down* CMP is difficult because the surface being polished is always in contact with the pad. With the *face-up* CMP scheme, polishing is given a bias depending on the rotational velocity ratios of the wafer and pad and therefore is much easier to control. Given a velocity ratio of $\omega_w / \omega_p = 1$, the theoretical model (Fig. 5) predicts more material removal at the center of the wafer for polishing with a stationary pad.

In the *face-up* CMP scheme, a fiber-optic sensor is used differentiate between the polished regions and the unpolished copper. Silicon and copper have different levels of reflectivity which correspond to different voltage outputs from the sensor. The end point sensor is situated about the center of the wafer and at the edge of the polishing pad, shown in Figure 9, and is able to detect regions of silicon "opening up."
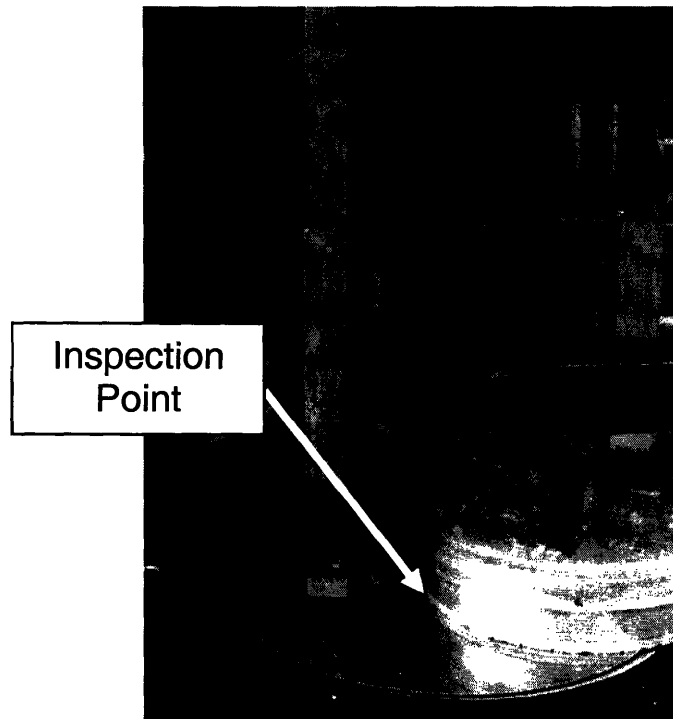

Figure 9: End point-sensor inspecting center of wafer.

At the point of opening, the sensor readings will immediately drop from a steady high voltage to an average voltage between copper and silicon. As polishing continues, the position of the cup can be controlled by maintaining the same averaged voltage output from the sensor.

4. Experimental Procedures

Figure 6 shows the prototype *face-up* CMP tool used to polish 100-mm blanket Cu wafers. Three separate experiments were conducted to verify the theoretical model of the *face-up* CMP. With a fixed pad, i.e., $v_{cc} = 0$, experiments were run with varying wafer-to-pad rotational velocity ratios of 1, 1.5, and 2. A blanket Cu wafer is shown in Figure 10 and the parameters of these experiments are listed in Table 1.
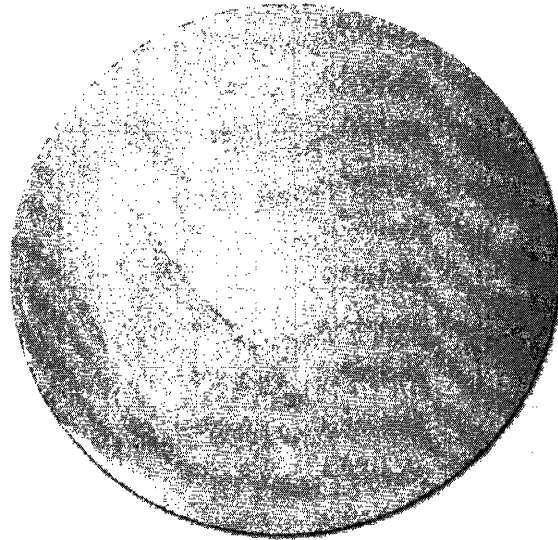
Figure 10: Unpolished copper blanket wafer.

Table 1. Material Properties.

Parameter	Value
Type of Cu Deposition	Electroplating
Thickness of Cu (nm)	1600
Ta/TaN Barrier Layer Thickness (nm)	15
Pad	IC1400
Slurry	iCue5001

For each test, the wafer-pad rotational velocity ratio was changed from 1 to 1.5 to 2, corresponding to experimental conditions in Tables 2, 3, and 4, respectively.

Table 2. Experimental Conditions for $\omega_w / \omega_p = 1$

Parameter	Value
Wafer Diameter (mm)	100
Pad Diameter (mm)	70
Nomial Pressure (kPa)	14
Wafer Rotational Velocity (rpm)	200
Pad Rotational Velocity (rpm)	200
Test Duration (s)	470

Table 3. Experimental Conditions for $\omega_w / \omega_p = 1.5$

Parameter	Value
Wafer Diameter (mm)	100
Pad Diameter (mm)	70
Nomial Pressure (kPa)	14
Wafer Rotational Velocity (rpm)	300
Pad Rotational Velocity (rpm)	200
Test Duration (s)	540

Table 4. Experimental Conditions for $\omega_w / \omega_p = 2$

Parameter	Value
Wafer Diameter (mm)	100
Pad Diameter (mm)	70
Nomial Pressure (kPa)	14
Wafer Rotational Velocity (rpm)	400
Pad Rotational Velocity (rpm)	200
Test Duration (s)	330

20

5. Results

Figure 11 shows still pictures from a video taken during polishing. Figure 12 is a schematic of a partially polished wafer.

(a)   (b)   (c)
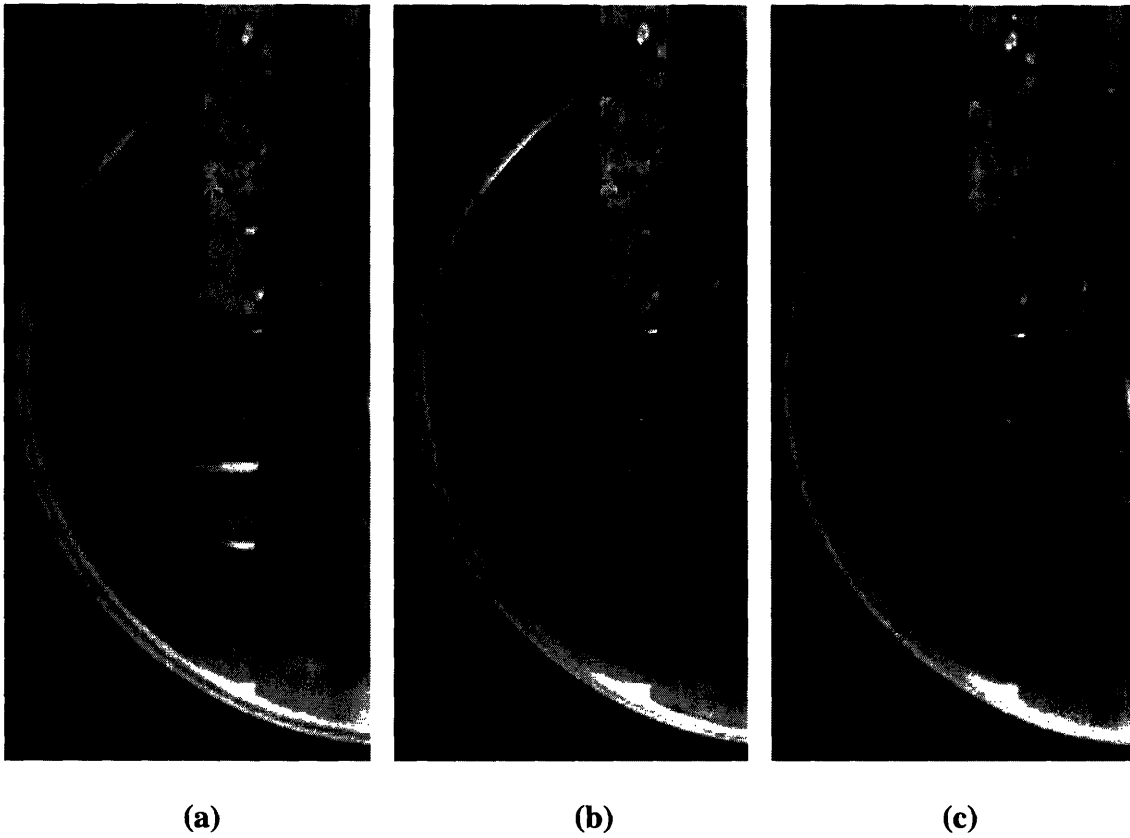
Figure 11: Copper blanket wafer at (a) t = 4min, (b) t = 4.5min, (c) and t = 5min, for the rotational velocity ratio of $\omega_w / \omega_p = 2$.
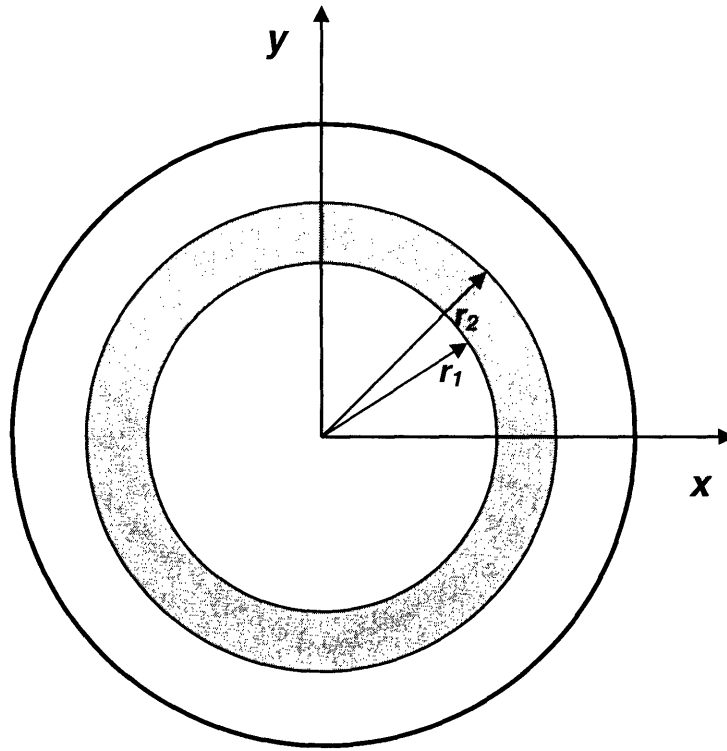
Figure 12: Coordinate system for the polished region.

The results of the three experiments are summarized in Tables 5, 6, and 7 for the velocity ratios 1, 1.5, and 2, respectively.

Table 5. Results of the $\omega_w / \omega_p = 1$ experiment.				
t, min	r_1, mm	r_2, mm	r_1 / r_w	r_2 / r_w
0	—	—		
6	20.5	20.5	0.41	0.41
6.5		23.3		0.47
7		30.8		0.62
7.5		36.3		0.73
7.8		38.4		0.77

Table 6. Results of the $\omega_w / \omega_p = 1.5$ experiment.

t, min	r_1, mm	r_2, mm	r_1 / r_w	r_2 / r_w
0	—	—		
5.5	14.7	21.8	0.29	0.44
6		29.4		0.59
6.5		35.3		0.71
7		38.8		0.78
7.5		41.2		0.82
8		42.9		0.86
8.5		44.1		0.88
9		45.3		0.91

Table 7. Results of the $\omega_w / \omega_p = 2$ experiment.

t, min	r_1, mm	r_2, mm	r_1 / r_w	r_2 / r_w
0	—	—		
3.66	39.3	39.3	0.79	0.79
4	33.0	44.6	0.66	0.89
4.5	25.9	47.8	0.52	0.96
5	19.2	49.1	0.38	0.98
5.5	16.5	50.00	0.33	1.00

Figure 13 shows the data from the three experiments recorded in Tables 5, 6, and 7. The data are plotted in dimensionless form, with normalized material removal rate versus the dimensionless radial position on the wafer.
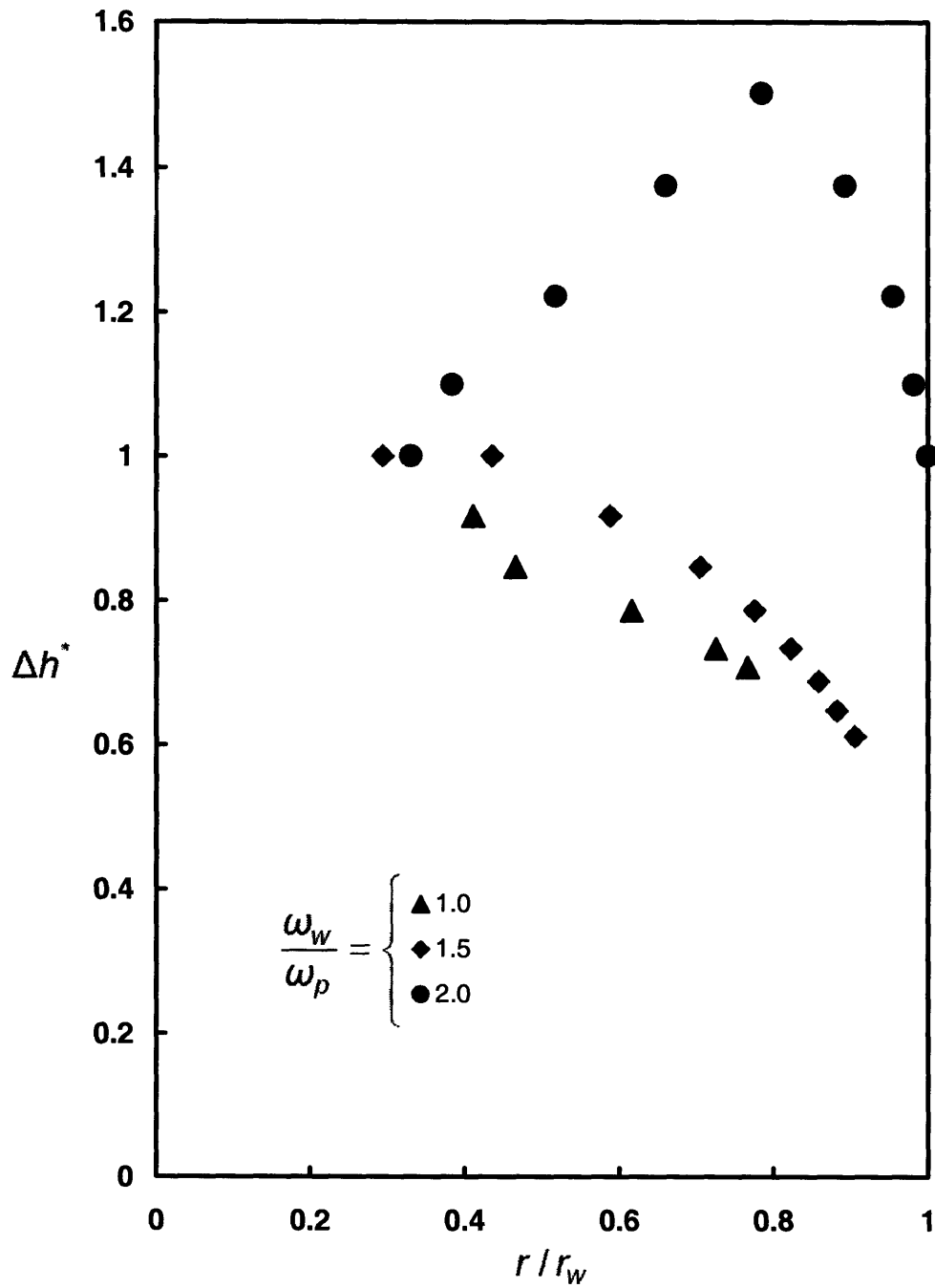
Figure 13: Experimental Δh^* versus r/r_w plots for three different ω_w/ω_p values.

6. Discussion

Figure 13 demonstrates a general trend of the way the wafers are polished. Though it does not completely correlate with values of the theoretical model in Fig. 5, it does show a resemblance. The wafer that was polished with a rotational velocity ratio of 1 exhibited a steeper, linear relation between material removed and the position of the polished region moving toward the edge of the wafer. The wafer polished with a rotational velocity of ratio 1.5 reveals a flat region around $r / r_w = 0.35$ and then quickly drops off, similar to the plateau seen in Fig. 5 for similar velocity ratios. Similarly, the rotational velocity ratio of 2 is shown to peak above unity for normalized material removal, which corresponds to a much faster polishing rate.

While the empirical data do not exactly fit with the theoretical model, it seems to follow the general trends that each velocity ratio appears to have. Velocity ratio of 1.0 appears to have a constant removal rate and can be observed in Fig. 13 to be fairly linear with respect to radial position and time. Velocity ratio of 1.5 favors polishing the center region almost all at once and then drop off rapidly as material removal slows down near the edge of the wafer. Finally, the velocity ratio 2:1 seems to agree with the theoretical values and has the highest material removal rate at a distance of $r_{cc} \approx r_p$, for a very slight overlap of the edge of the pad and the center of the wafer.

The polishing however was not as uniform as theoretically modeled. For the velocity ratios 1 and 1.5, the copper should have been removed starting from the center and gradually remove more and more copper toward the edge. In actuality, the copper on the wafer was first completely polished away *near* the edge of the wafer in a concentric ring around the center. The wafer polishes symmetrically otherwise and the edge that moves outward appears to follow the general trend predicted by the theoretical model.

One consideration as to why the wafer is not completely polishing at the center could be the uniformity of polishing rates of the pad. The slurry is being fed through evenly distributed holes in the pad and therefore in the analysis, it is assumed constant throughout. It is also noted that the very edge of the pad does not behave the same way as the center of the pad, which is why there should be a slight overlap of the edge of the pad over the center of the wafer. It may turn out that the edge effects of the pad are

25

larger than previously thought, making the effective radius of the pad, r_p, smaller than the assumed value.

Another potential problem may that the pressure distribution under the pad was perhaps not uniform as assumed in the theoretical model. For simplicity, the theoretical analysis assumes that both the pressure and the Preston constant are uniform under the pad since the pad is smaller than the cup. If the pressure distribution of the pad over the wafer is non-uniform, then experimental data would not necessarily correlate with the theoretical model.

7. Conclusions

A working prototype *face-up* CMP tool has successfully been completed. Polishing experiments conducted on the *face-up* CMP machine appear to correspond at least qualitatively with the theoretical model. Discrepancies between experimental data and the theoretical model could potentially be due to non-uniform loading of the polishing pad and or uneven distribution of slurry under the pad due to the edge effects. Despite the discrepancies between the theoretical and the experimental values, empirical values suggest the theoretical model used to describe the *face-up* CMP tool is basically valid.

References

[1] Noh, K., 2005, "Modeling of Dielectric Erosion and Copper Dishing in Copper Chemical-Mechanical Polishing," Ph.D. thesis, Department of Mechanical Engineering, MIT, Cambridge, MA.

[2] Lai, J.-Y., 2001, "Mechanics, Mechanisms, and Modeling of the Chemical Mechanical Polishing Process," Ph.D. thesis, Department of Mechanical Engineering, MIT, Cambridge, MA.

[3] Preston, F.W., 1927, "The Theory and Design of Plate Glass Polishing Machines," *J. Soc Glass Technology*, vol. 11, pp. 214-256.